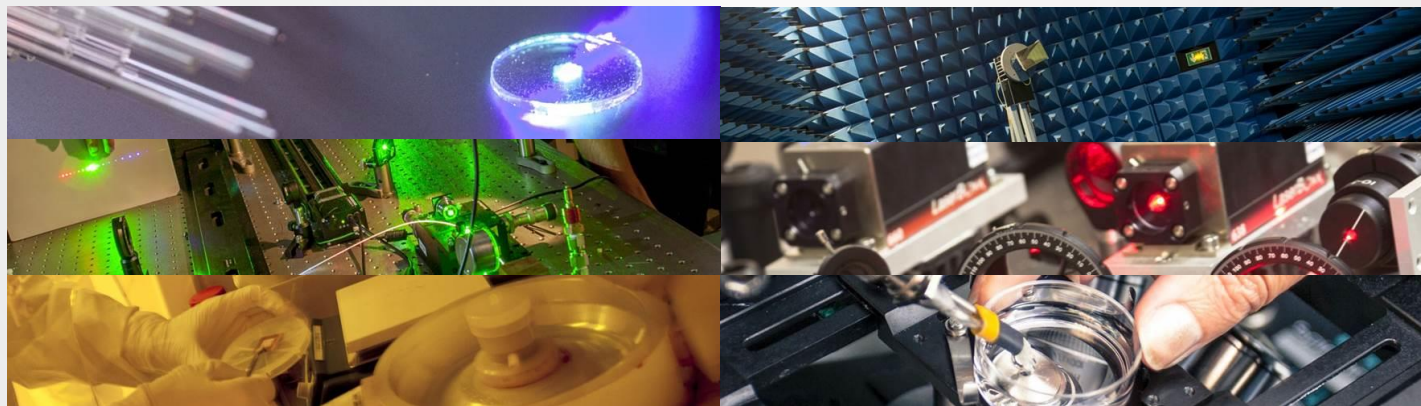
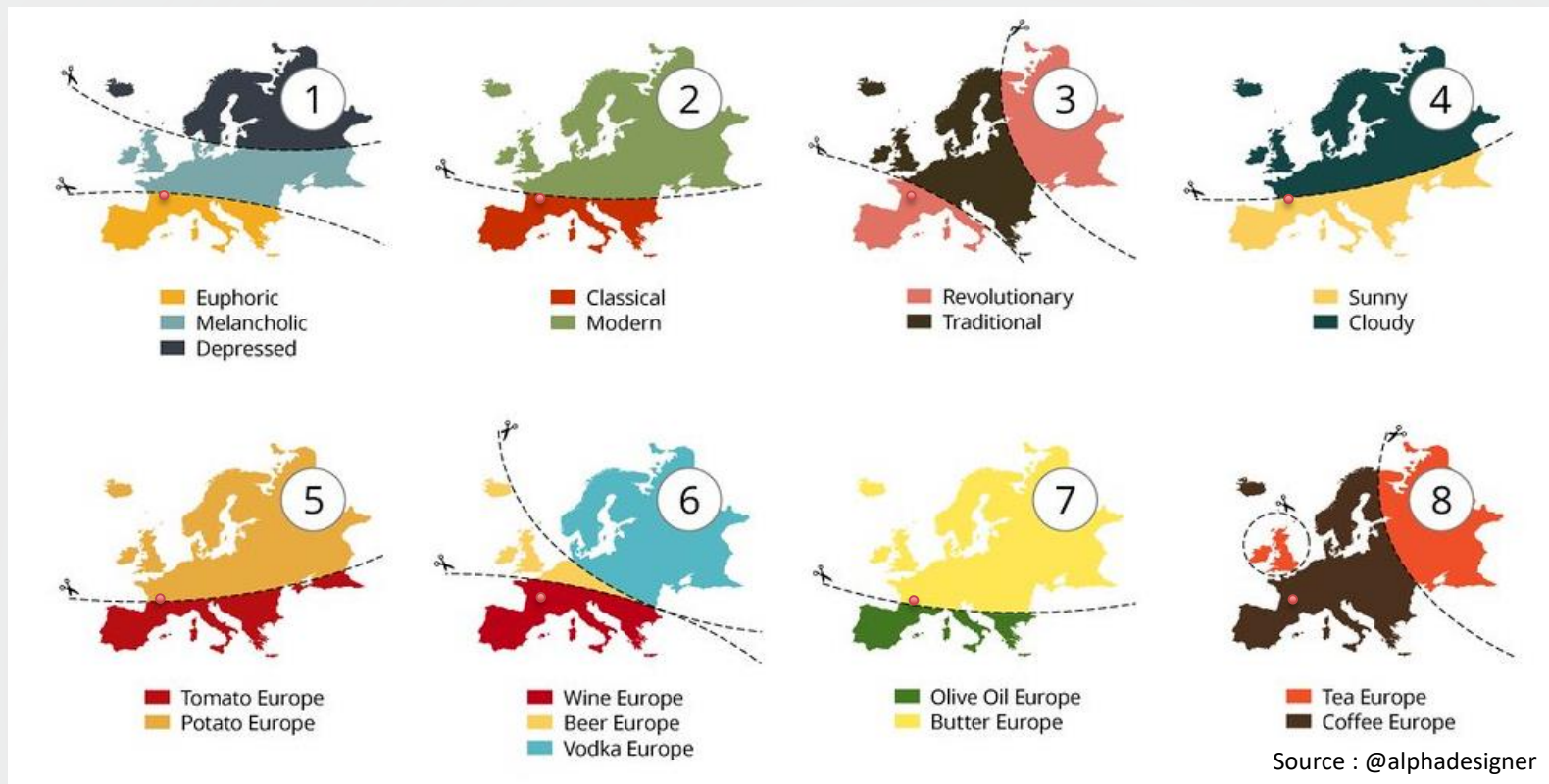


Microwave and millimeter-wave computational imaging

Thomas Fromentèze
Xlim and Collaborations

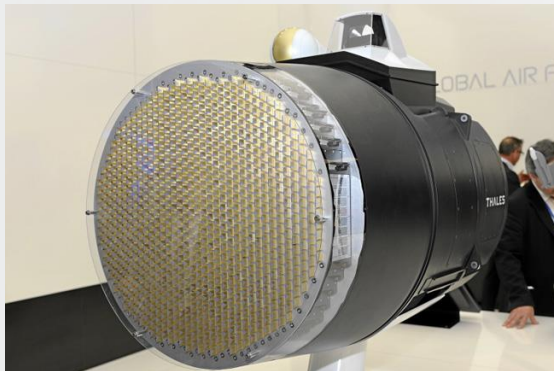




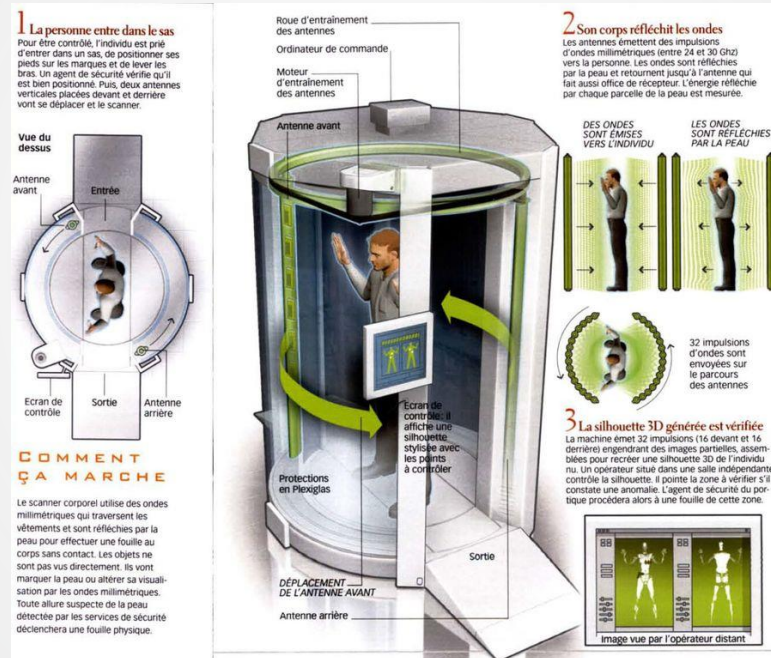


Limits of conventional imaging systems

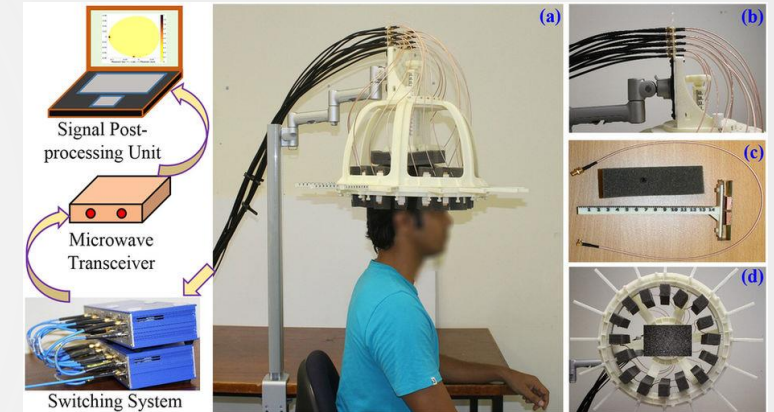
Resolution – Frame rate - Sensitivity



<https://omnirole-rafale.com/avionique/rbe2/>



<https://www.science-et-vie.com/archives/le-scanner-corporel-22514>

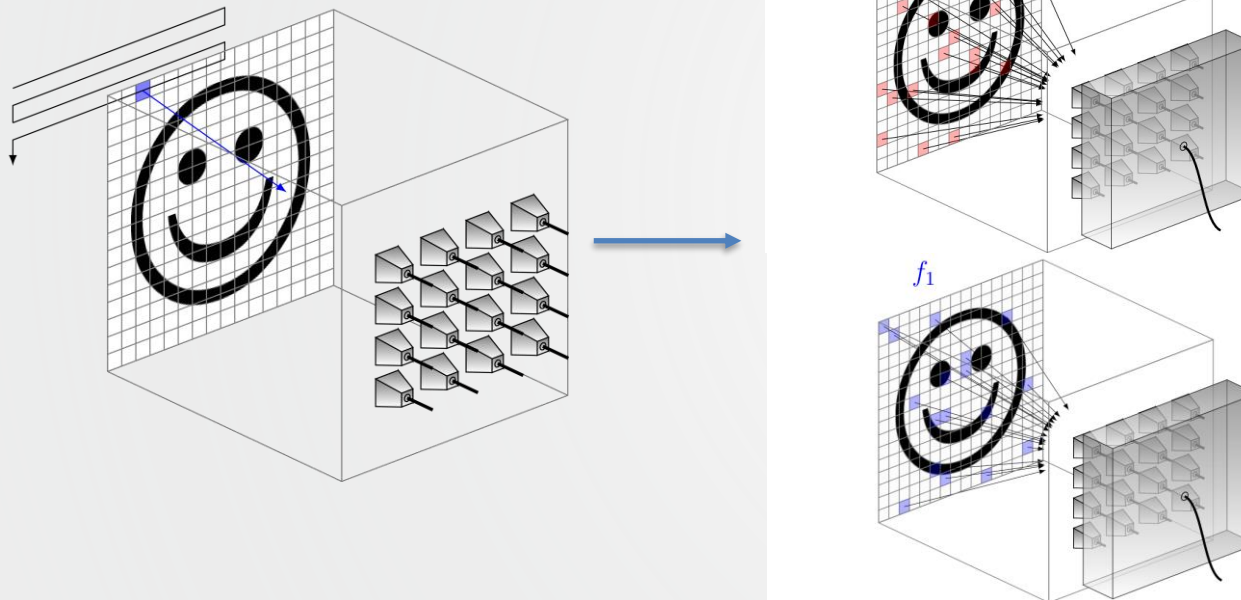


Mobashsher, Ahmed Toaha, and A. M. Abbosh. "On-site rapid diagnosis of intracranial hematoma using portable multi-slice microwave imaging system." Scientific reports, 2016



Computational imaging

Computational method: The spatial information is encoded in the physical layer



Building Three-Dimensional Images Using a Time-Reversal Chaotic Cavity

Gabriel Montaldo, Delphine Palacio, Mickael Tanter, and Mathias Fink

Science

Current Issue First release papers Archive About Submit manuscript

HOME > SCIENCE > VOL. 340, NO. 6134 > 3D COMPUTATIONAL IMAGING WITH SINGLE-PIXEL DETECTORS

REPORT

f t in e x

3D Computational Imaging with Single-Pixel Detectors

B. SUN, M. P. EDGAR, B. BOWMAN, L. E. VITTERT, S. WELSH, A. BOWMAN, AND M. J. PADGETT [Authors Info & Affiliations](#)

SCIENCE · 17 May 2013 · Vol 340, Issue 6134 · pp. 844-847 · DOI: 10.1126/science.1234454

1957 463

CHECK ACCESS

C. R. Physique 11 (2010) 37–43



ELSEVIER

Contents lists available at ScienceDirect

Comptes Rendus Physique

www.sciencedirect.com



Propagation and remote sensing / Propagation et télédétection

Focusing and amplification of electromagnetic waves by time reversal in a leaky reverberation chamber

Focalisation et amplification d'ondes électromagnétiques par retournement temporel dans une chambre semi-réverbérante

Mathieu Davy^{a,*}, Julien de Rosny^a, Jean-Christophe Joly^b, Mathias Fink^a

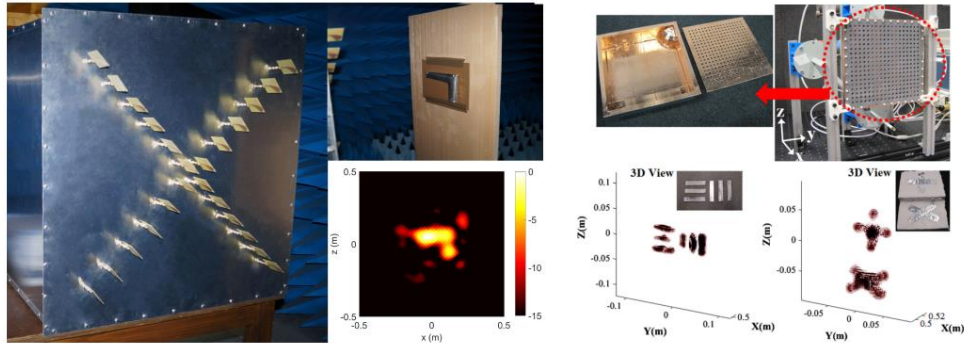
^a Institut Langevin, ESPCI ParisTech, CNRS UMR 7587, laboratoire ondes et acoustique, 10, rue Vauquelin, 75231 Paris cedex 05, France

^b Centre d'études de Gramat, 46500 Gramat, France



Background: The rise of computational microwave and millimeter imaging

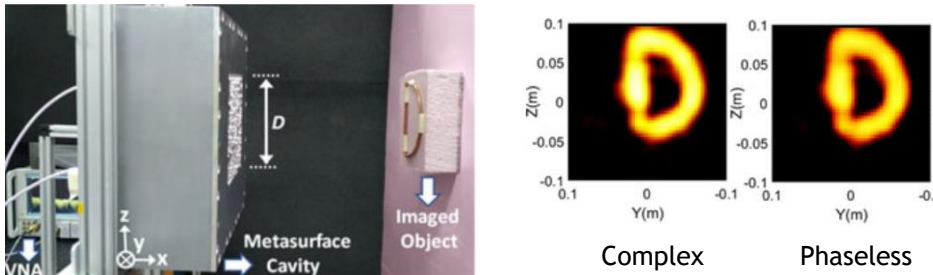
2015 - Scalar multistatic/MIMO imaging



Fromenteze, T., Yurduseven, O., Imani, M. F., Gollub, J., Decroze, C., Carsenat, D., & Smith, D. R. (2015). Computational imaging using a mode-mixing cavity at microwave frequencies. *Applied Physics Letters*, 106(19), 194104.

Fromenteze, T., Kpré, E. L., Carsenat, D., Decroze, C., & Sakamoto, T. (2016). Single-shot compressive multiple-inputs multiple-outputs radar imaging using a two-port passive device. *IEEE Access*, 4, 1050-1060.

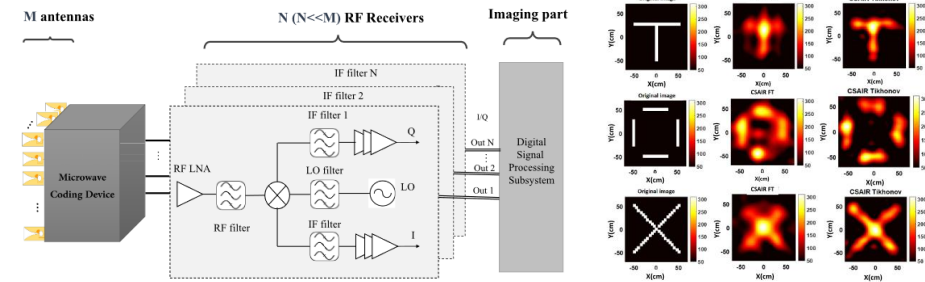
2016 - Phaseless imaging



Fromenteze, T., Liu, X., Boyarsky, M., Gollub, J., & Smith, D. R. (2016). Phaseless computational imaging with a radiating metasurface. *Optics express*, 24(15), 16760-16776.

Yurduseven, O., Fromenteze, T., Marks, D. L., Gollub, J. N., & Smith, D. R. (2017). Frequency-diverse computational microwave phaseless imaging. *IEEE Antennas and Wireless Propagation Letters*, 16, 2808-2811.

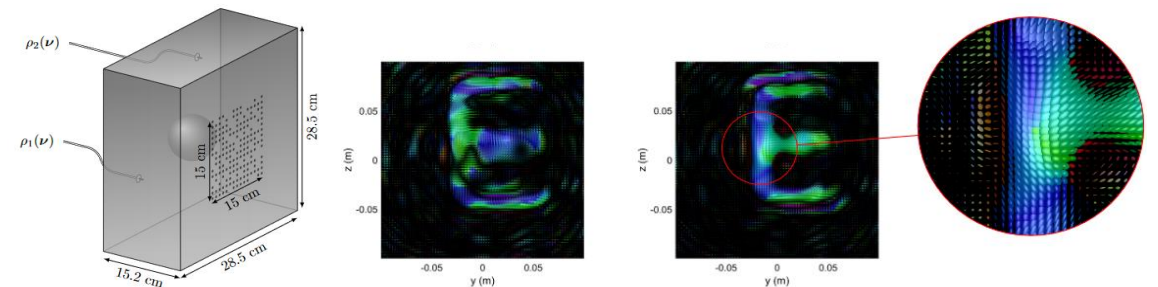
2016 - Interferometric imaging



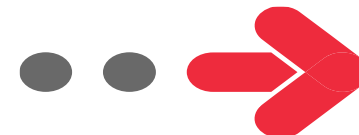
Kpré, E. L., & Decroze, C. (2016, October). Synthetic aperture interferometric imaging using a passive microwave coding device. In *2016 IEEE Conference on Antenna Measurements & Applications (CAMA)* (pp. 1-4). IEEE.

Kpré, E., Decroze, C., Mouhamadou, M., & Fromenteze, T. (2018). Computational imaging for compressive synthetic aperture interferometric radiometer. *IEEE Transactions on Antennas and Propagation*, 66(10), 5546-5557.

2017 Polarimetric imaging



Fromenteze, T., Yurduseven, O., Boyarsky, M., Gollub, J., Marks, D. L., & Smith, D. R. (2017). Computational polarimetric microwave imaging. *Optics express*, 25(22), 27488-27505.





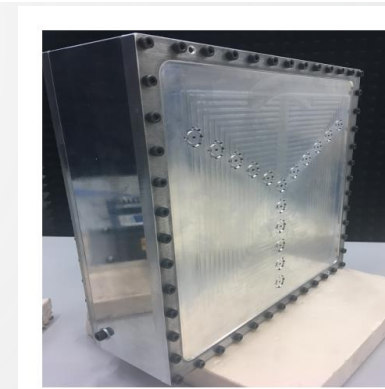
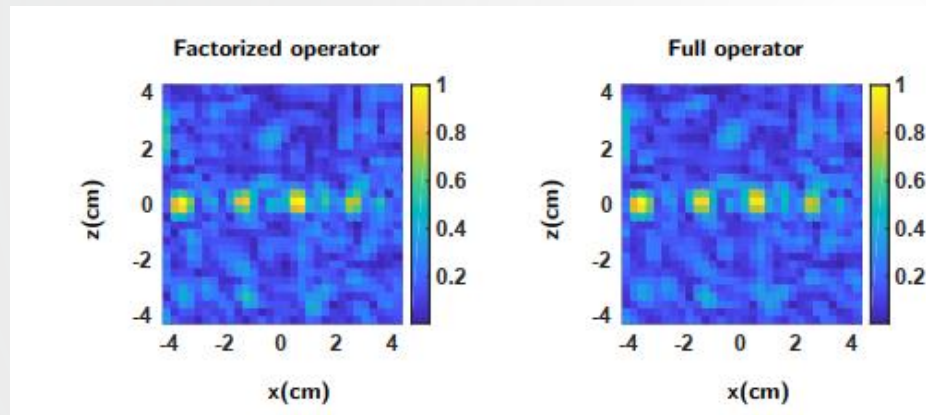
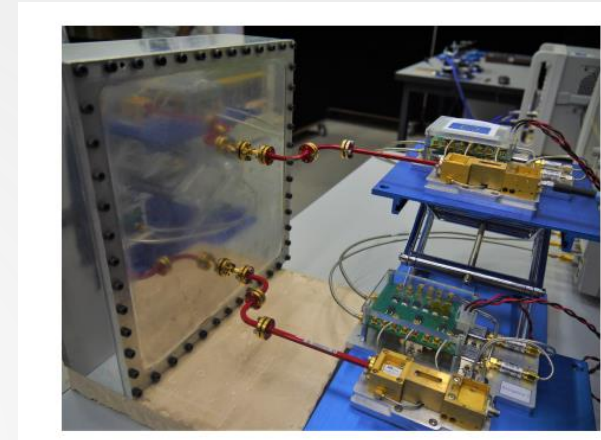
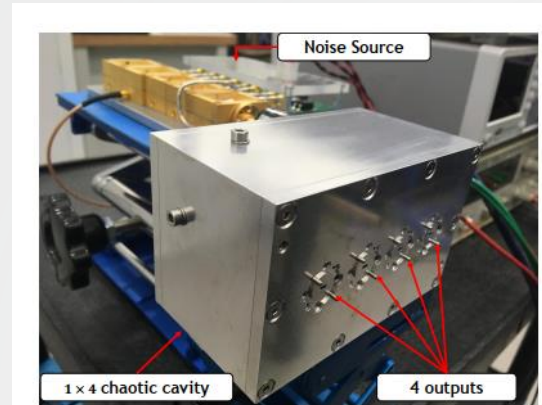
Recent (non exhaustive) works



Interferometric computational imaging - W band

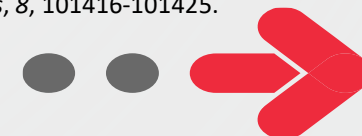


Sana Abid



ANR Pixel - Collaboration MC2 Tech. CEA Gramat

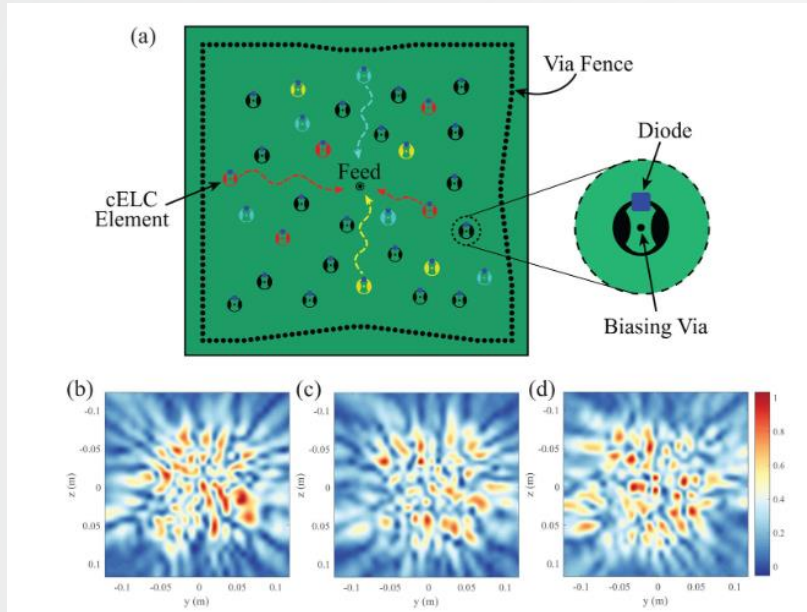
Abid, S., Decroze, C., Mouhamadou, M., & Fromenteze, T. (2020). Enhancing millimeter-wave computational interferometric imaging. *IEEE Access*, 8, 101416-101425.



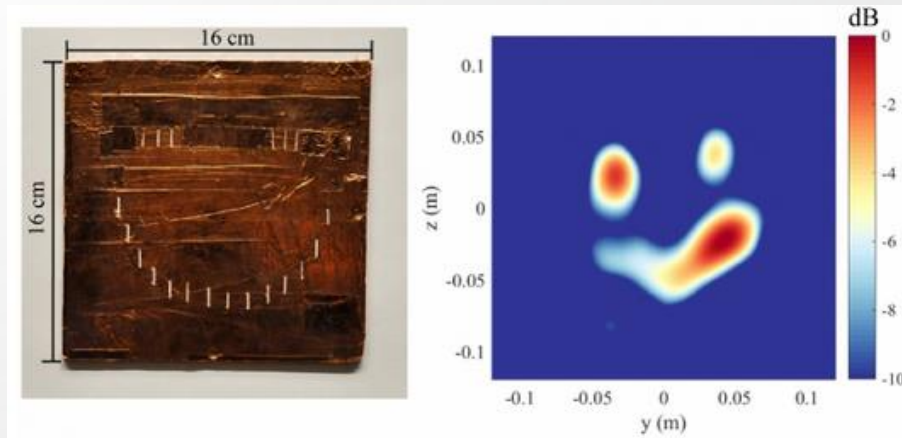
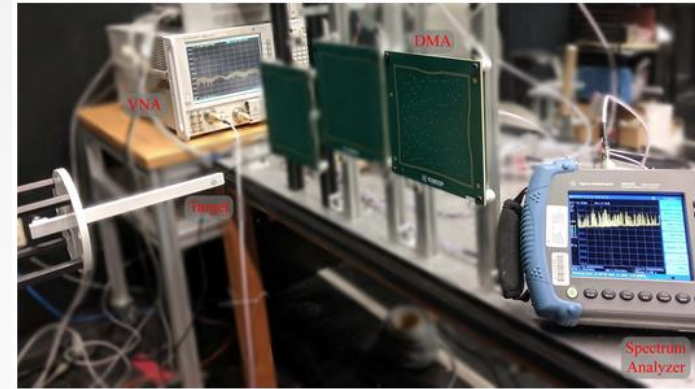
Phaseless computational imaging - K band



Aaron Diebold
Duke University



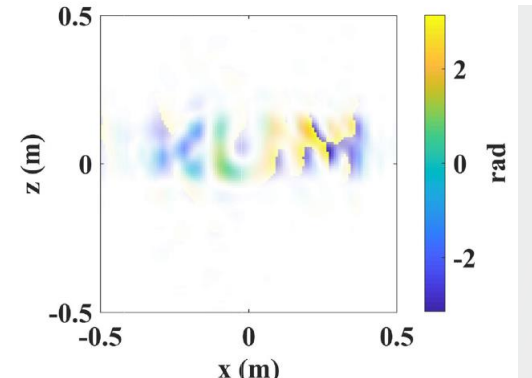
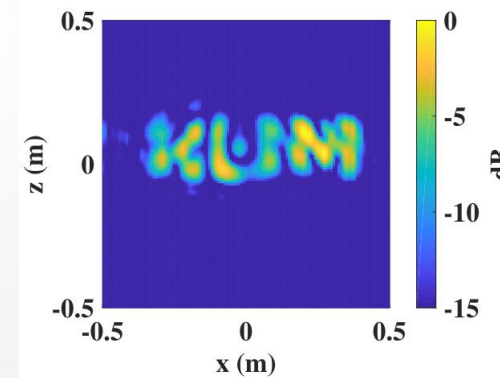
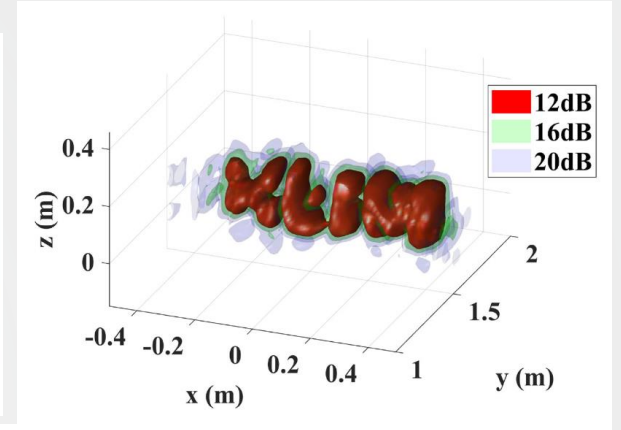
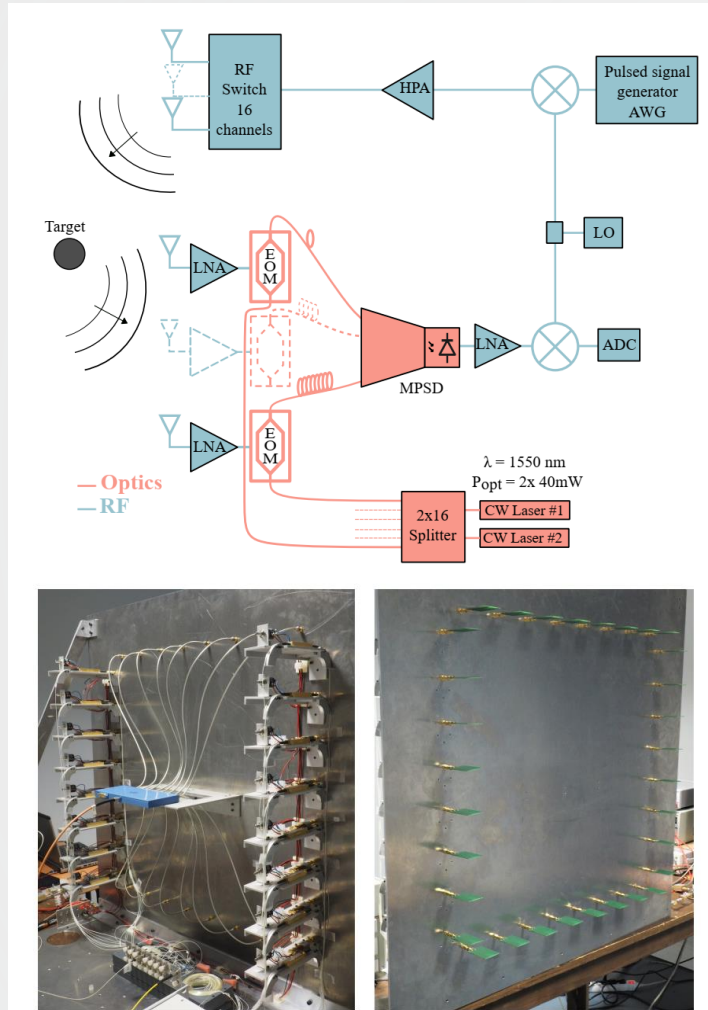
Diebold, A. V., Imani, M. F., Fromenteze, T., Marks, D. L., & Smith, D. R. (2020). Passive microwave spectral imaging with dynamic metasurface apertures. *Optica*, 7(5), 527-536.



Microwave photonic radar imaging - C band



Fabien Berland



ANR Obiwam - Collaboration C2N, MC2, Vectrawave, STM

Berland, F., Fromenteze, T., Boudescoque, D., Di Bin, P., Elwan, H. H., Aupetit-Berthelemot, C., & Decroze, C. (2020). Microwave Photonic MIMO Radar for Short-Range 3D Imaging. *IEEE Access*, 8, 107326-107334.

thomas.fromenteze@unilim.fr





Focus on a recent work in direct link with the GDR Complex

PHYSICAL REVIEW APPLIED

Highlights Recent Subjects Accepted Collections Authors Referees Search Press About Editorial Team

Spatiotemporal Analysis of Electromagnetic Field Coherence in Complex Media

Thomas Fromenteze, Matthieu Davy, Okan Yurduseven, Yann Marie-Joseph, and Cyril Decroze
Phys. Rev. Applied **17**, 054039 – Published 24 May 2022

Twitter Facebook More

Article References No Citing Articles PDF HTML Export Citation

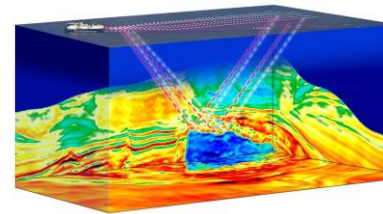
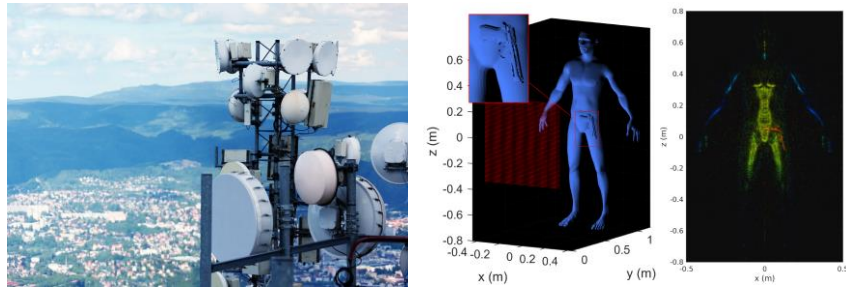
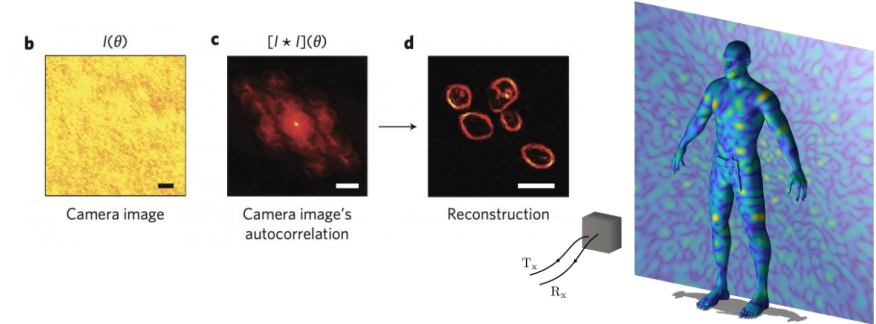
Related work

Mounaix, M., & Carpenter, J. (2019)
Control of the temporal and polarization
response of a multimode fiber.
Nature communications, 10(1), 1-8.





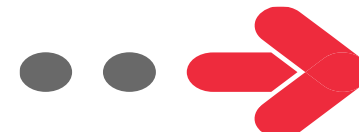
Problem: Digital processing is generally based on approximations



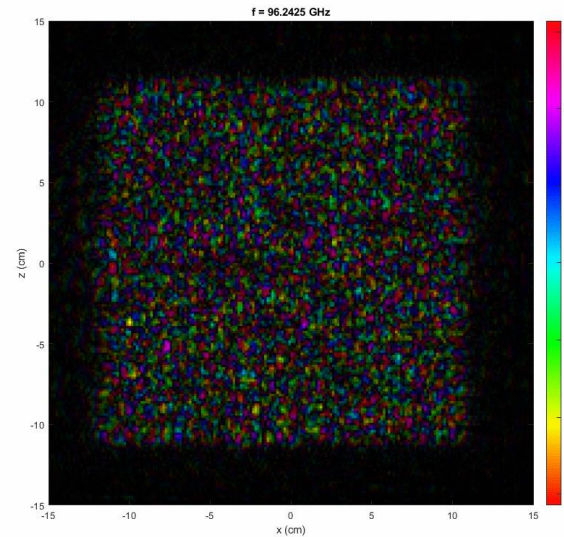
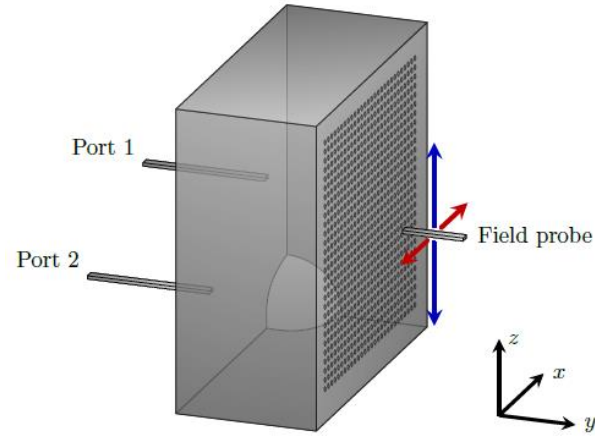
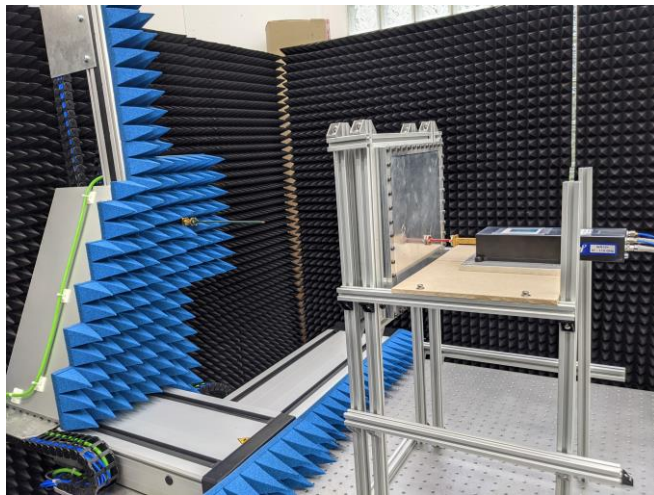
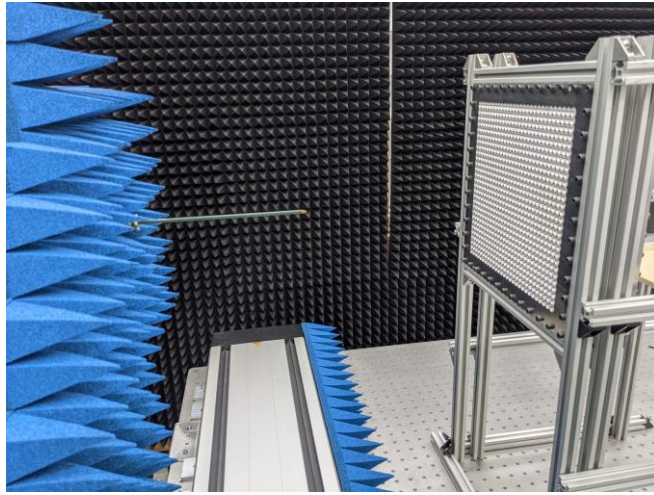
Coherent fields

Diffuse fields

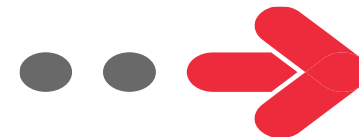
Sources: mvg-world.com - beteirconl.cluster026.hosting.ovh.net - trends.aeroexpo.online - unilim.fr/pages_perso/thomas.fromenteze - faradayshielding.com.au - lkb.upmc.fr/opticalimaging/imaging/ cgg.com



Background: : Radiation of frequency-diverse and spatially diffuse fields

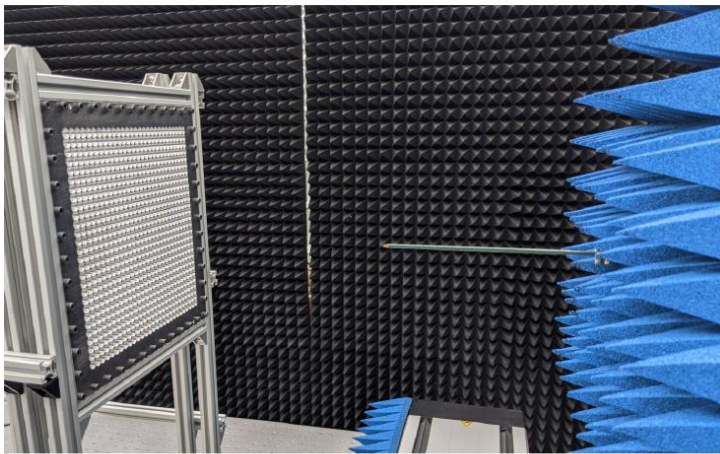
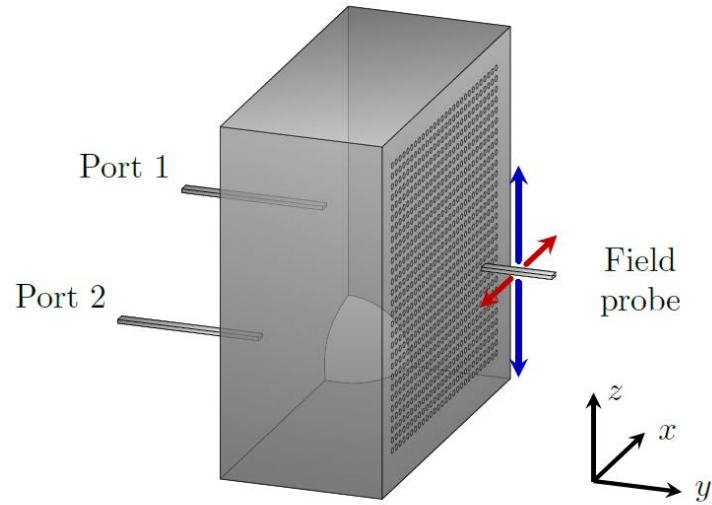


Frequency band: 70-100 GHz
Dimensions: 251 x 66 x 251 mm³
Feeding: Two z-polarized WR-10 ports
Radiation: 28 x 28 circular irises





Background: Radiation of frequency-diverse and spatially diffuse fields



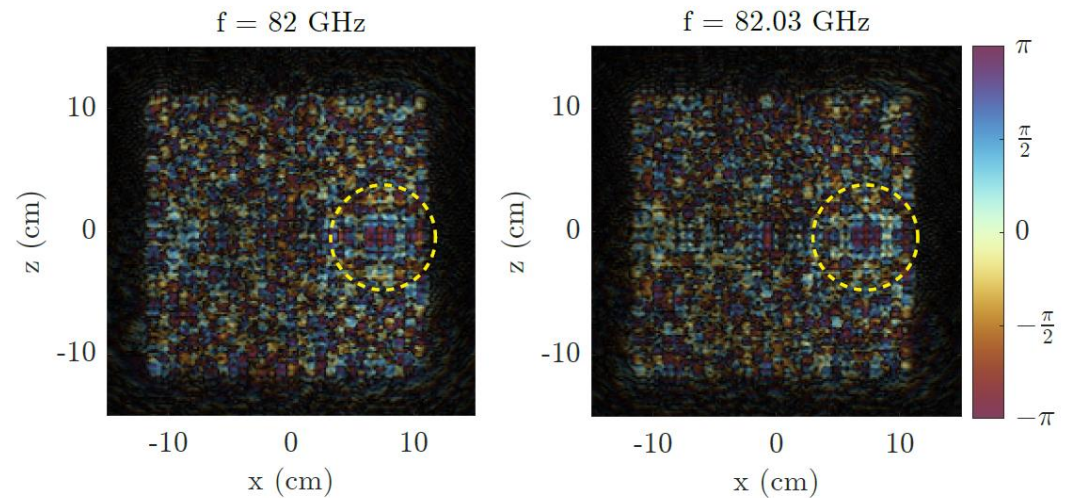
Frequency band: 70-100 GHz

Dimensions: 251 x 66 x 251 mm³

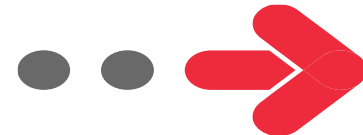
Feeding: Two z-polarized WR-10 ports

Radiation: 28 x 28 circular irises

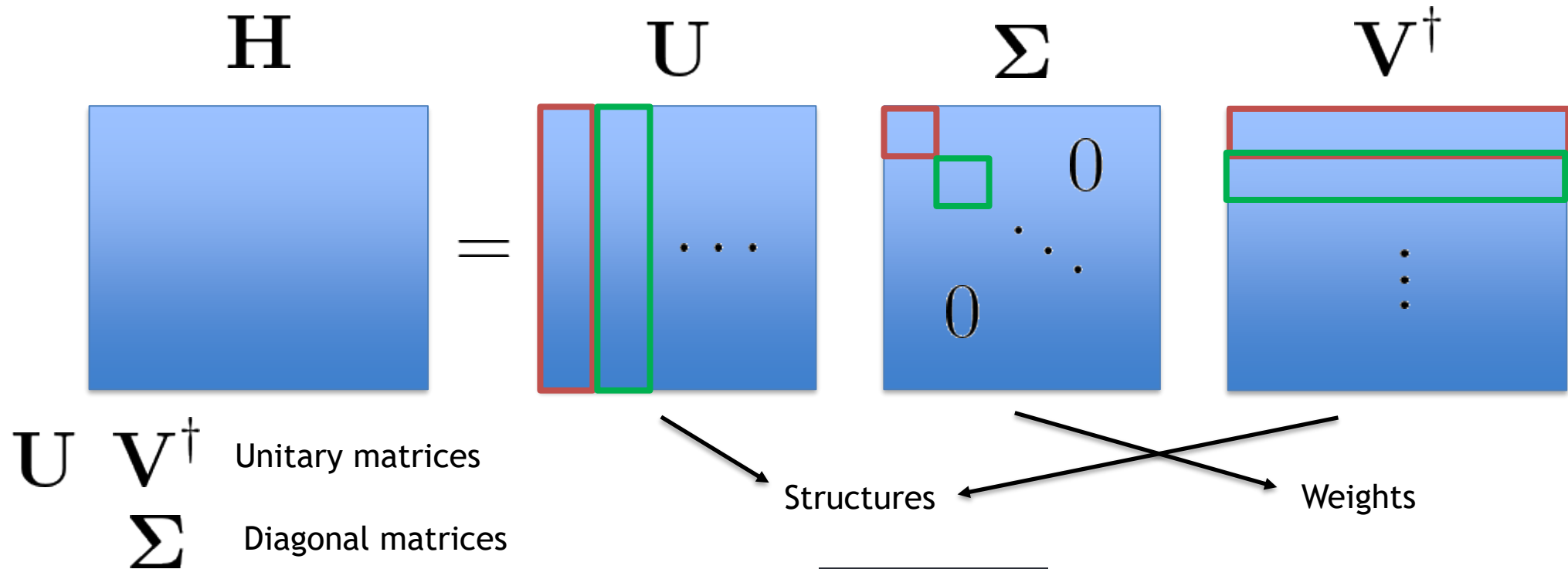
Direct coupling with the feeding probe



Contributions coherent in time and space that should be removed



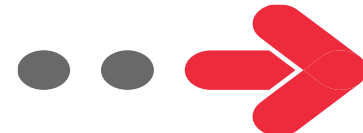
Method: Feature extraction by Singular Value Decomposition



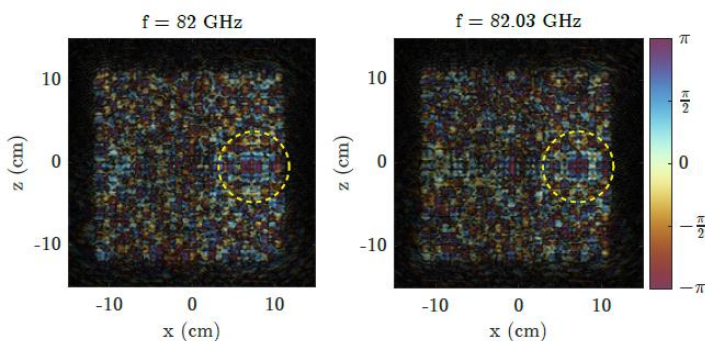
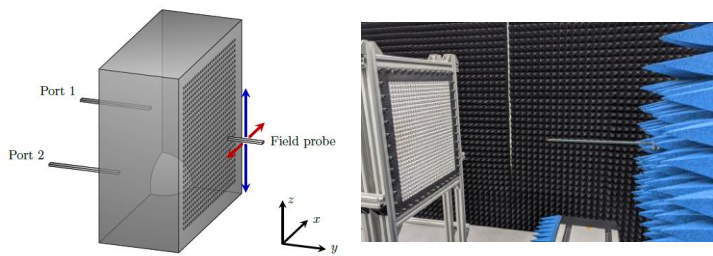
Matlab `[U,S,V] = svd(H);`

Julia `U, S, V = svd(A);`

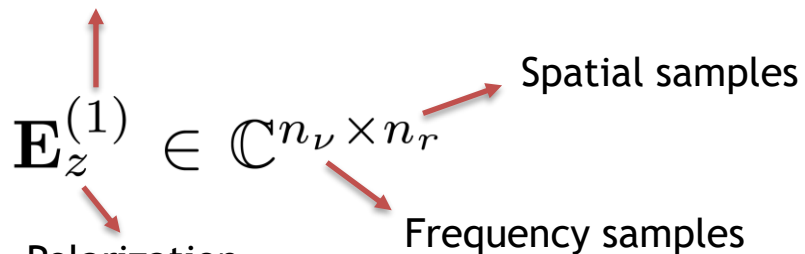
Python-Numpy `U, S, V = np.linalg.svd(H, full_matrices=True)`



Method: Feature extraction by Singular Value Decomposition



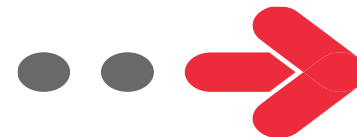
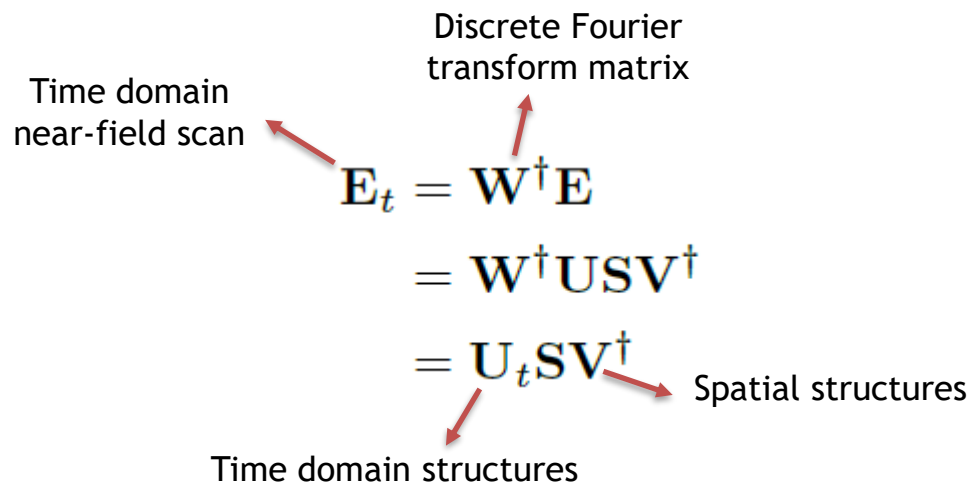
Feeding port index



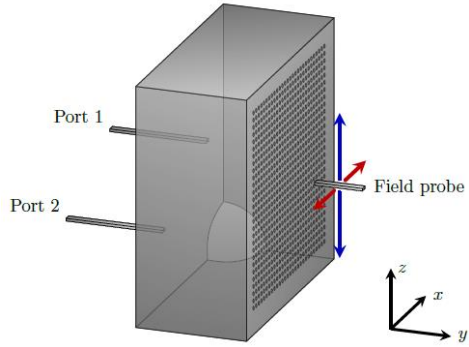
Factorization of a near-field matrix

$$\mathbf{E} = \sum_n \sigma_n \mathbf{u}_n \mathbf{v}_n^\dagger \rightarrow \begin{array}{l} \mathbf{u}_n \in \mathbb{C}^{n_\nu \times 1} \rightarrow \text{Frequency domain structures} \\ \mathbf{v}_n \in \mathbb{C}^{n_r \times 1} \rightarrow \text{Spatial structures} \end{array}$$

Effect of a Fourier transform

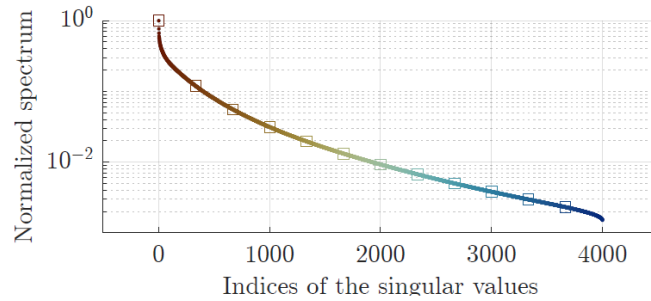


Results: Time domain structures

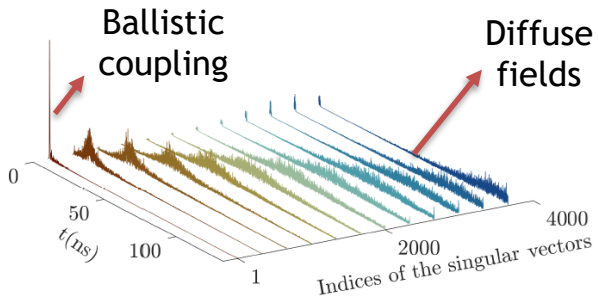


$$\begin{aligned} \mathbf{E}_t &= \mathbf{W}^\dagger \mathbf{E} \\ &= \mathbf{W}^\dagger \mathbf{U} \mathbf{S} \mathbf{V}^\dagger \\ &= \mathbf{U}_t \mathbf{S} \mathbf{V}^\dagger \end{aligned}$$

Singular value spectrum

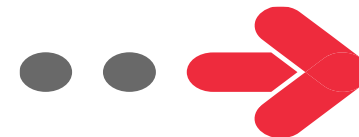
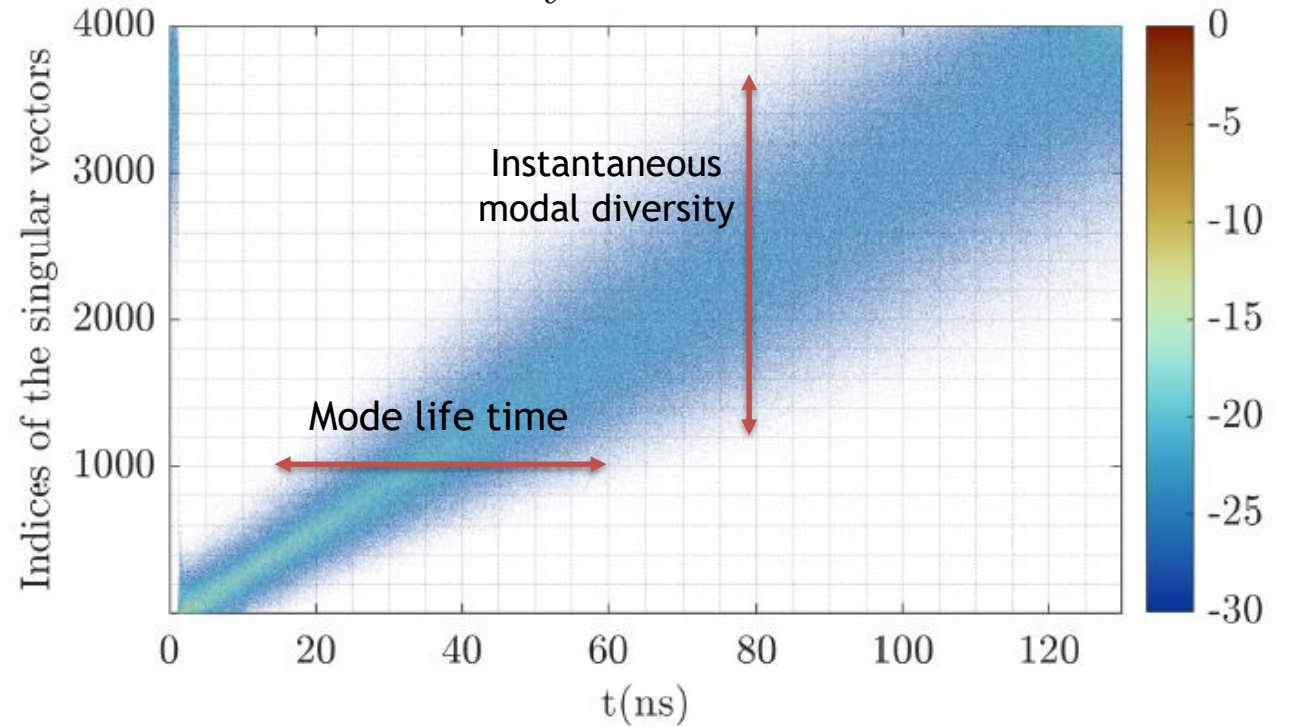


Time domain singular vectors

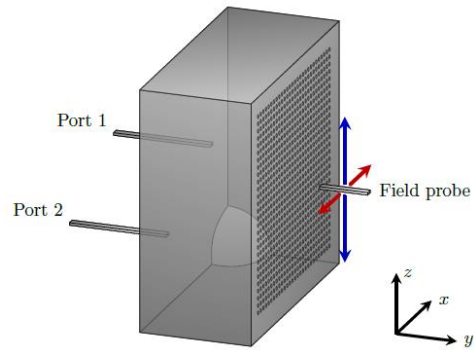


Discrete Fourier transform matrix

$$\mathbf{U}_t = \mathbf{W}^{-1} \mathbf{U}$$



Results: Spatial structures



$$\begin{aligned} \mathbf{E}_t &= \mathbf{W}^\dagger \mathbf{E} \\ &= \mathbf{W}^\dagger \mathbf{U} \mathbf{S} \mathbf{V}^\dagger \\ &= \mathbf{U}_t \mathbf{S} \mathbf{V}^\dagger \end{aligned}$$

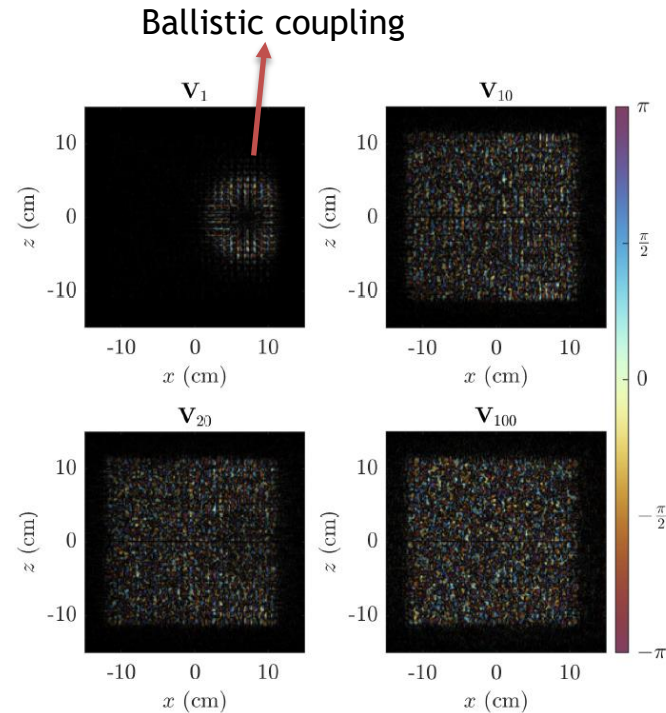
Matrix of spatial singular vectors

Extraction of the spatial singular vectors

$$\mathbf{v}_n = \text{vec}(\mathbf{V}_n)$$

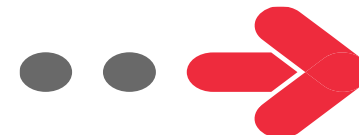
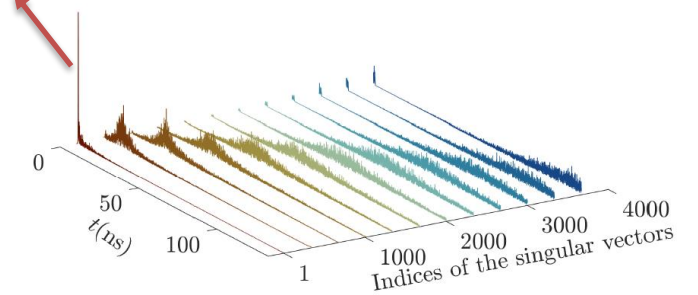
Reconstruction of the spatial structures by “de-vectorization”

Reshaped spatial singular vectors



Ballistic coupling

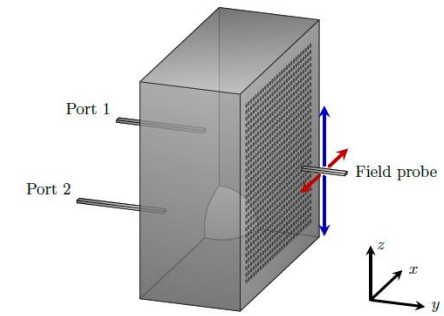
Associated time domain singular vectors



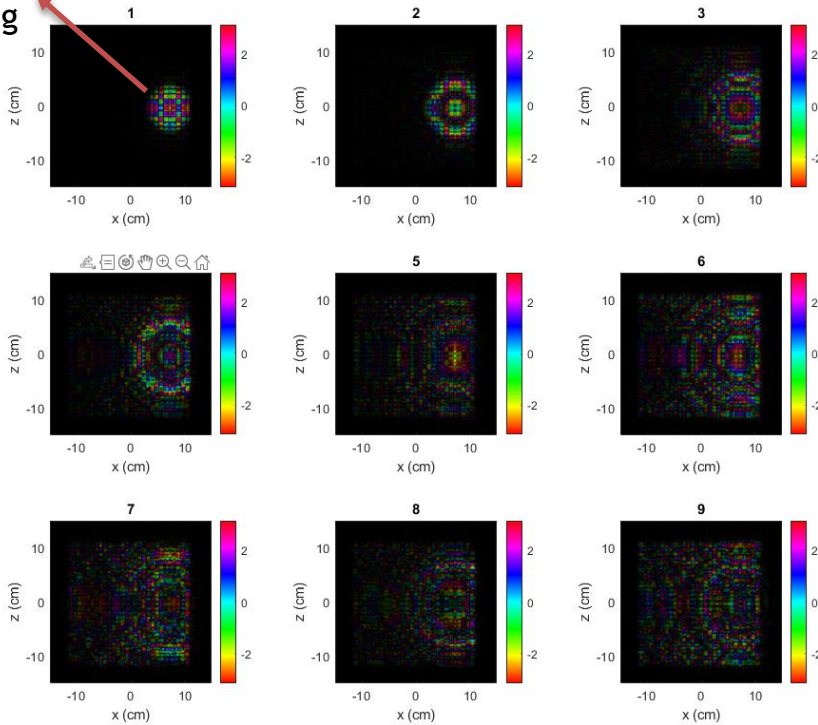


Results: On the effect of polarization

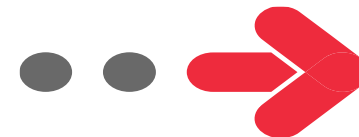
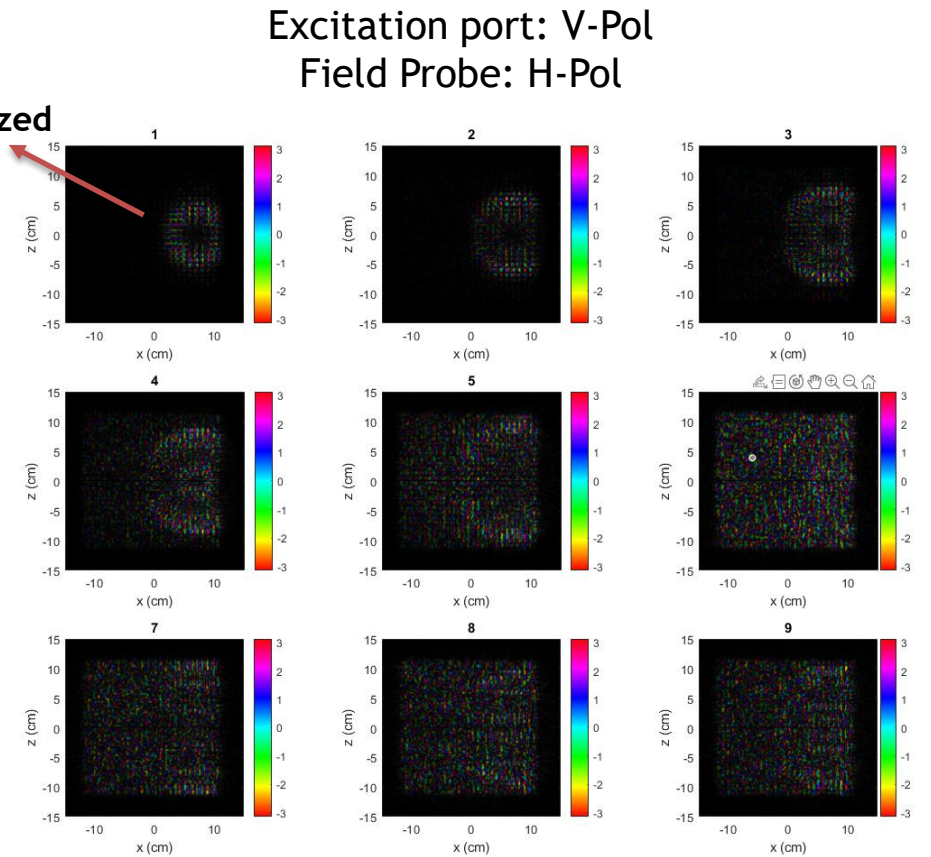
Observation of the first spatial singular vectors



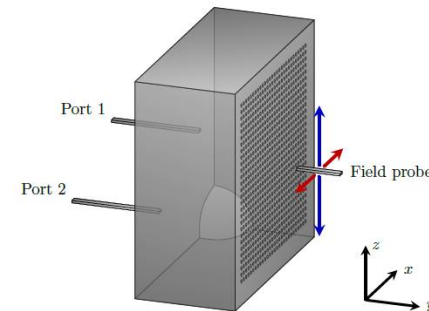
Ballistic
co-polarized
coupling



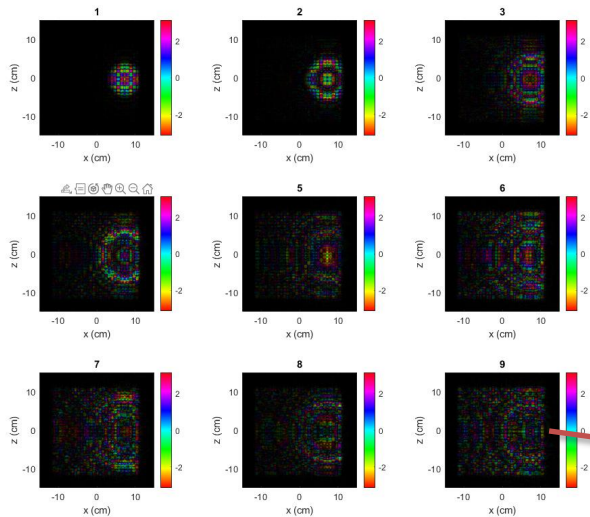
Ballistic
cross-polarized
coupling



Results: On the effect of polarization

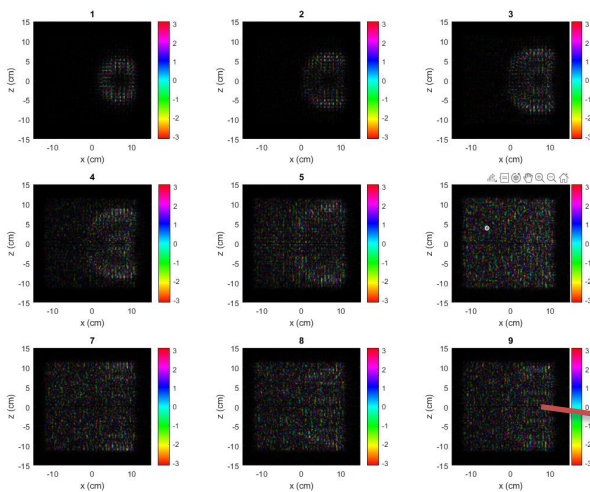


Co-polarized measurements

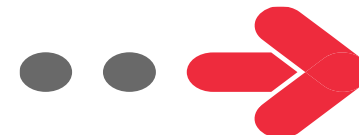
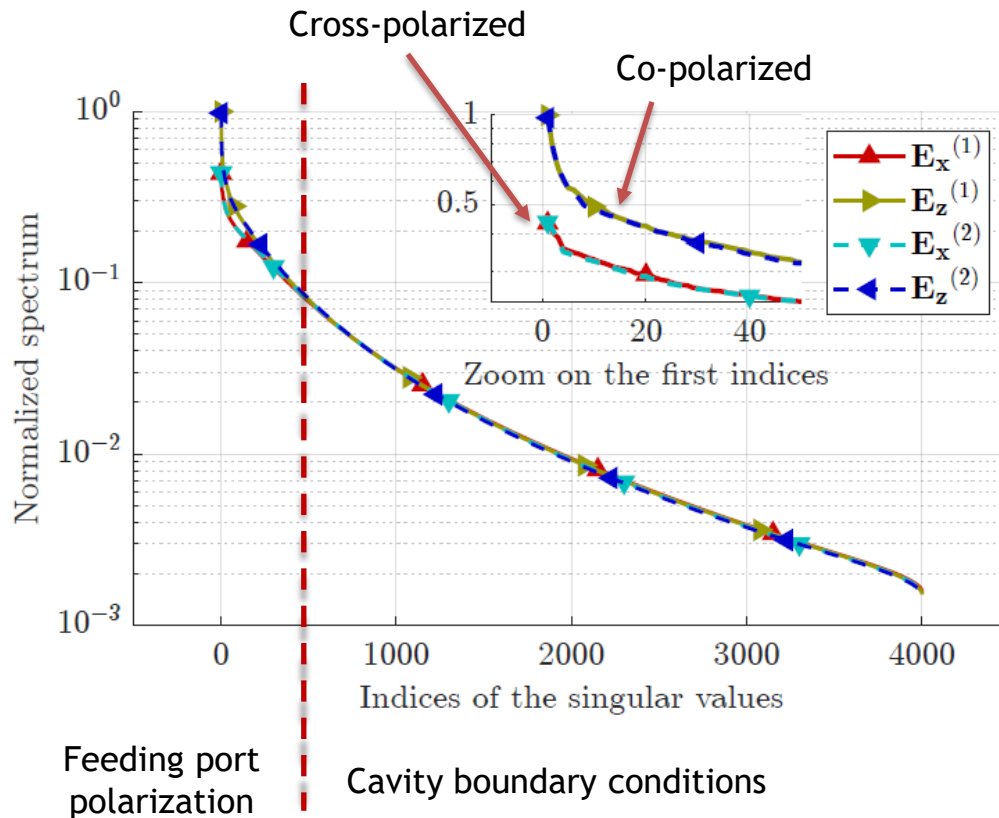


Remain spatially coherent

Cross-polarized measurements

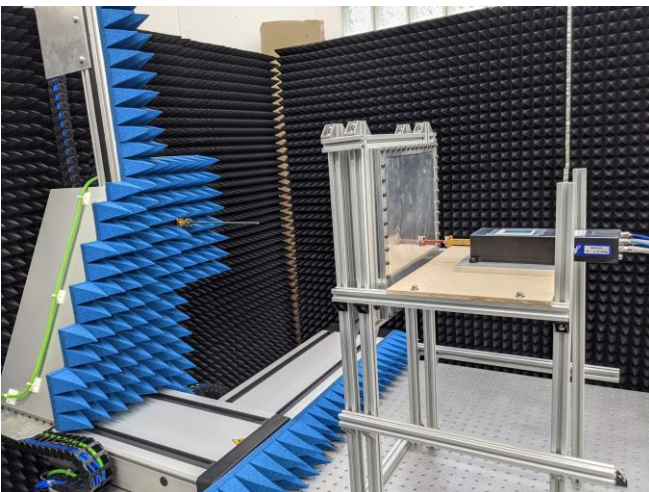
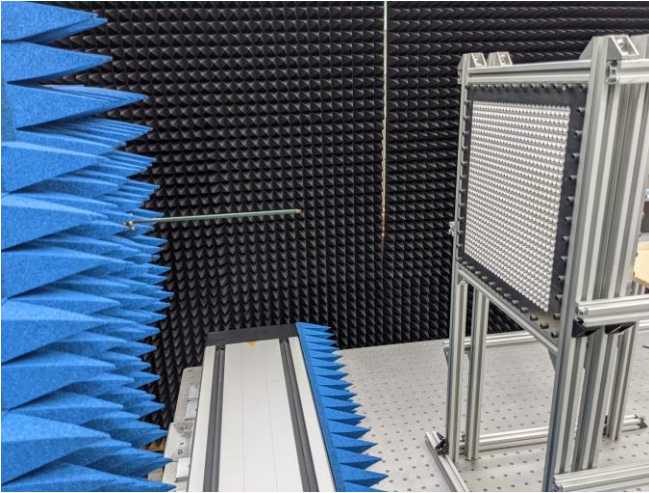


Closer to a diffuse field distribution



Results: Application to computational imaging

Antenna localization



1. Near-field to dipole conversion

$$\mathbf{m} = \frac{2}{i2\pi\nu\mu_0} \int \hat{\mathbf{n}} \times \mathbf{E}_{\text{tan}} da$$

2. Computation of the radiated field

$$\mathbf{E}(\mathbf{r}_j) = -Z_0 k^2 \sum_i (\hat{\mathbf{r}}_{ij} \times \mathbf{m}_i) \frac{e^{-ikr_{ij}}}{4\pi r_{ij}} \left(1 - \frac{i}{k r_{ij}}\right)$$

3. Forward problem: Measurement of the transfer function

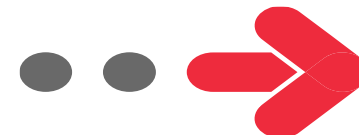
Feeding port index

$$\mathbf{s}^{(q)} = \mathbf{E}_0 \boldsymbol{\rho}^{(q)}$$

4. Inverse problem: Source localization

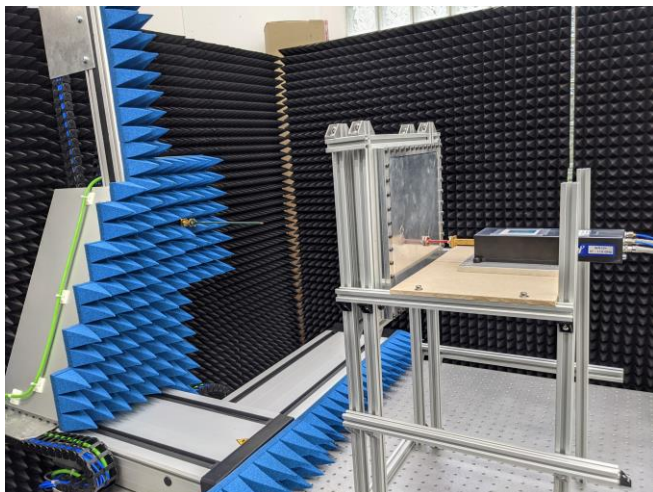
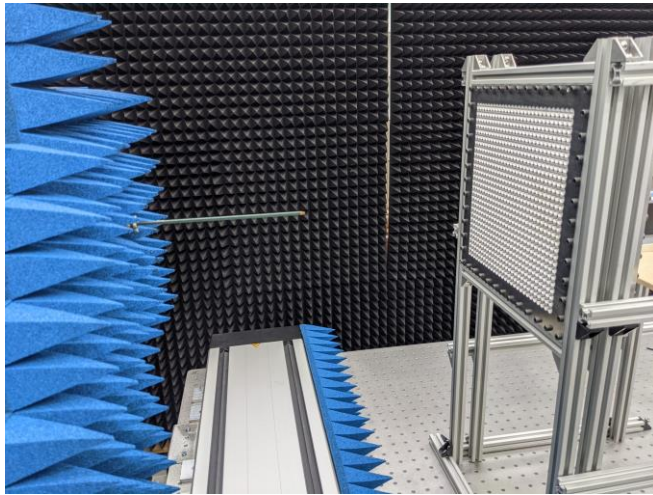
$$\hat{\boldsymbol{\rho}}_m^{(q)} = \mathbf{E}_m^\dagger \mathbf{s}^{(q)} = \mathbf{E}_m^\dagger \mathbf{E}_0 \boldsymbol{\rho}^{(q)}$$

Removing the m first singular values and vectors



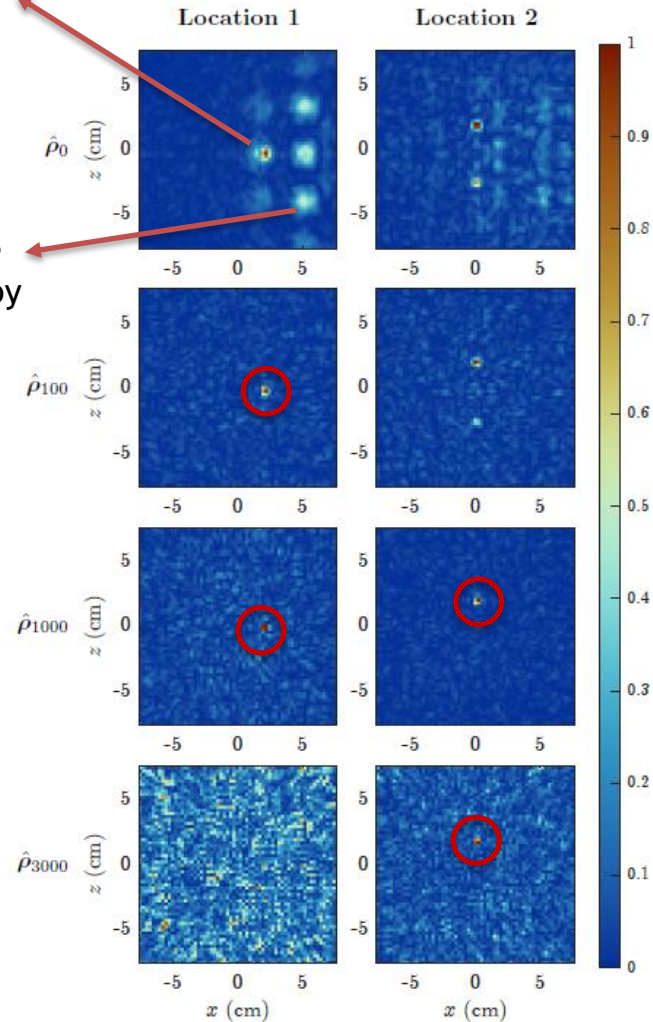
Results: Application to computational imaging

Antenna localization



Source

Diffraction of the ballistic coupling by the iris array

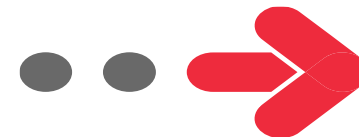


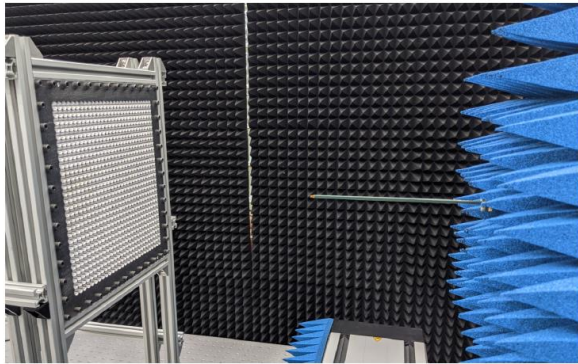
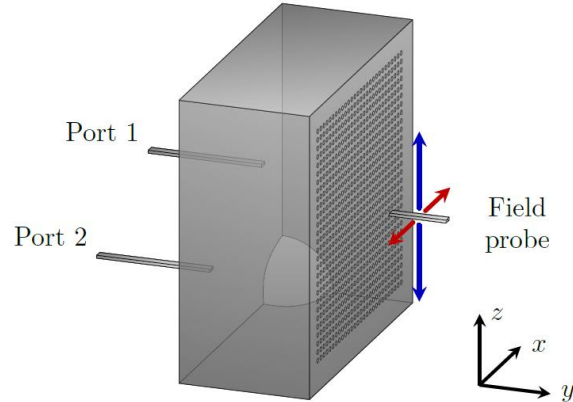
Filtering of the m most coherent subspaces

$$\mathbf{E}_{x,z}^{[m]} = \sum_{n=m+1}^{n_\nu} \sigma_n \mathbf{u}_n \mathbf{v}_n^\dagger$$

Inverse problem:
Source localization

$$\hat{\rho}_m^{(q)} = \mathbf{E}_m^\dagger \mathbf{s}^{(q)} = \mathbf{E}_m^\dagger \mathbf{E}_0 \rho^{(q)}$$



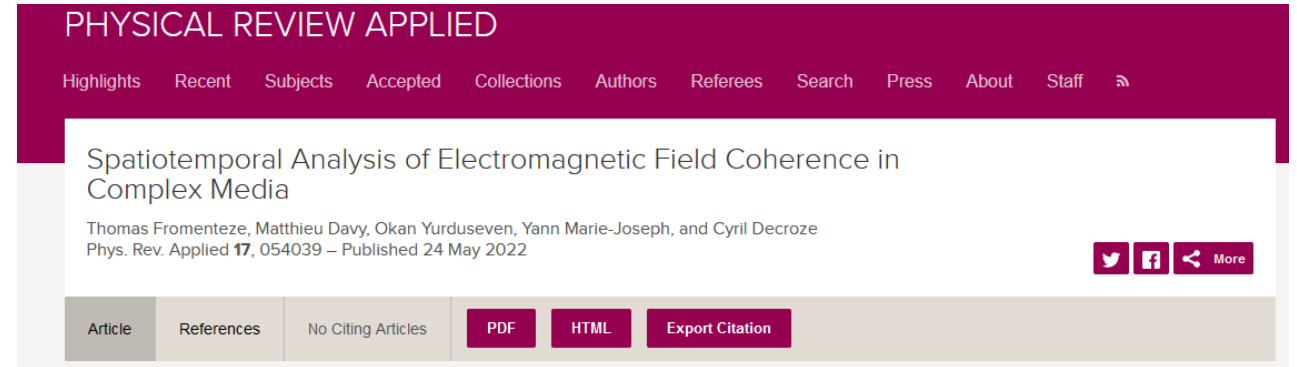


Related work

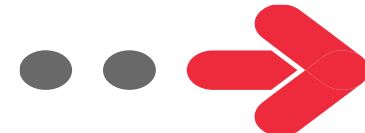
Mounaix, M., & Carpenter, J. (2019)
Control of the temporal and polarization
response of a multimode fiber.
Nature communications, 10(1), 1-8.

Conclusion

Extended version published in
Physical Review Applied

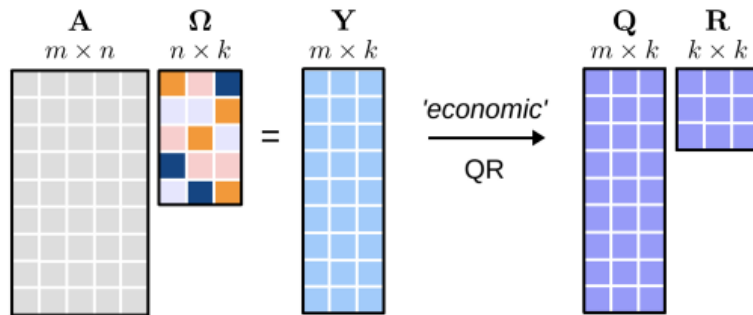


What is different from this presentation?
Introduction of coherence metrics
Evolution of spatial vs temporal coherence
SVD-based filtering vs Time-gating

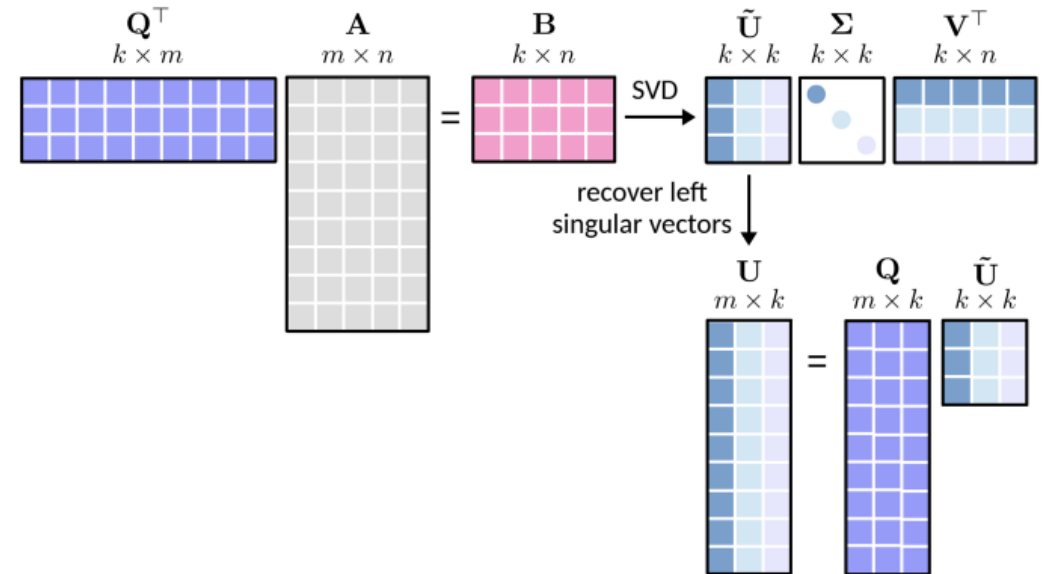


Implementation with large matrices : Randomized SVD

1. Multiplication by a random matrix et QR decomposition



2. Multiplication by the initial matrix and SVD



Sources : <https://towardsdatascience.com/intuitive-understanding-of-randomized-singular-value-decomposition-9389e27cb9de>